Publication VII

Piippo, A., Salomäki, J., and Luomi, J. “Signal injection in sensorless PMSM drives equipped with inverter output filter.” *IEEE Transactions on Industry Applications*. (In press)

Signal Injection in Sensorless PMSM Drives Equipped With Inverter Output Filter

Antti Piippo, *Non-member, IEEE,* Janne Salomäki, *Member, IEEE,* and Jorma Luomi *Member, IEEE*

***Abstract*—The paper proposes a hybrid observer for sensorless control of permanent magnet synchronous motor drives equipped with an inverter output LC filter. An adaptive full-order observer is augmented with a high-frequency signal injection method at low speeds. The only measured quantities are the inverter phase currents and the dc-link voltage. The effects of the LC filter on the signal injection are investigated, and it is shown that the filter is not an obstacle to using signal injection methods. The proposed method allows sensorless operation in a wide speed range down to zero speed. Experimental results are given to confirm the effectiveness of the proposed method.**

***Index Terms*—Inverter output filter, permanent magnet motors, sensorless control, signal injection.**

I. Introduction

Problems may be encountered in ac motor drives due to the non-sinusoidal voltage produced by a pulse-width modulated (PWM) inverter. The high rate of change of the voltage (i.e. high $\mathrm{d}u/\mathrm{d}t$) may cause excessive voltage stresses in the stator winding insulations. It may also cause leakage currents through the parasitic capacitances of the stator winding and produce bearing currents. Voltage harmonics cause acoustic noise and power losses; the losses caused by eddy currents are a special concern in high-speed solid-rotor motors.

A common approach to overcome these problems is to use an inverter output filter [1]–[4]. An LC filter, having the resonance frequency below the switching frequency, is a typical choice for the filter topology if a nearly sinusoidal output voltage is required. However, this kind of heavy filtering makes the motor control more difficult. A conventional scalar control method is usually employed, but when better control performance is needed, a vector control method must be used. For vector control, the filter dynamics should be taken into account.

Various methods have been proposed for the vector control of variable-speed drives equipped with an LC filter. Methods based on feedforward action and sliding mode control have been used for compensating the effects of the filter in a sensorless permanent magnet synchronous motor (PMSM) drive in [2]. Direct measurement of the stator voltages and currents has been used for obtaining feedback signals for the current control and the speed and position estimation in a sensorless PMSM drive [3]. A feedforward current controller has been used in a speed-sensored synchronous reluctance motor drive with an LC filter [4]. For induction motor drives equipped with an LC filter, vector control methods based on cascaded controllers have been proposed in [5], [6].

Due to the LC filter, the voltages and currents at the motor terminals differ from those of the inverter output. Frequency converters are equipped with measurements of output currents, and output voltages are also known. For vector control, however, the corresponding quantities at the motor terminals are needed. In [2]–[6], the motor voltages or currents are measured by additional sensors, requiring hardware modifications in the motor drive. If the motor quantities are estimated instead, as in [7]–[9] for induction motor drives, the additional measurements are avoided and a filter can be added to an existing drive. Recently, a similar method has been proposed for sensorless PMSM drives [10].

The above mentioned sensorless techniques are based on fundamental-excitation methods, which do not allow sustained operation at low speeds. As a solution to this problem, high-frequency (HF) signal injection methods have been developed for sensorless PMSM drives without a filter [11]–[14]. However, such methods have not been previously applied to ac motor drives equipped with an inverter output LC filter. It is not obvious how well the rotor position can be estimated from the response of the system to the injected HF signal when an LC filter is connected between the inverter output and the PMSM. In addition, the resonance frequency of the LC filter complicates the selection of the HF excitation frequency.

In this paper, a hybrid observer is proposed where a speed-adaptive full-order observer [10] is augmented with a pulsating high-frequency (HF) signal injection technique at low speeds. The effect of the inverter output LC filter on the signal injection is investigated, and the problems caused by the filter on the signal injection are addressed. It is shown that signal injection methods are feasible even with the filter if the frequency of the injected voltage signal is suitably chosen. For the compatibility of the signal injection method, the dynamics of the system are analyzed in frequency domain. The validity of the proposed hybrid observer is shown by means of simulations and laboratory experiments.

II. Filter and Motor Models

Fig. 1 shows a PMSM drive system equipped with an LC filter. The inverter output voltage $\mathbf{u}_A$ is filtered by the LC filter, resulting in a nearly sinusoidal stator voltage $\mathbf{u}_s$. The inverter output current $\mathbf{i}_A$ and the dc-link voltage u_{dc} are the only measured quantities.

This work was financially supported by ABB Oy and Walter Ahlström foundation.

Antti Piippo is with ABB Oy, Drives, P.O. Box 184, FI-00381 Helsinki, Finland (e-mail: antti.piippo@fi.abb.com). Janne Salomäki is with Konecranes PLC, P.O. Box 661, FI-05801 Hyvinkää, Finland. Jorma Luomi is with Helsinki University of Technology, Department of Electrical Engineering, P.O. Box 3000, FI-02015 TKK, Finland.

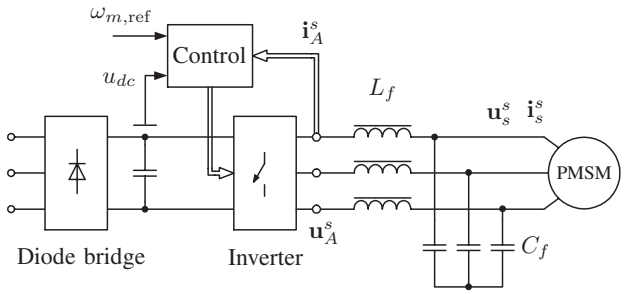

Fig. 1. PMSM drive system equipped with three-phase LC filter. Superscript s denotes the stator reference frame.

The PMSM and the LC filter are modeled in the d-q reference frame fixed to the rotor. The d axis is oriented along the permanent magnet flux, whose angle in the stator reference frame is θ_m in electrical radians. The stator voltage equation is

$$\mathbf{u}_s = R_s\mathbf{i}_s + \dot{\boldsymbol{\psi}}_s + \omega_m\mathbf{J}\boldsymbol{\psi}_s \tag{1}$$

where $\mathbf{u}_s = [\,u_{sd}\;\; u_{sq}\,]^T$ is the stator voltage, $\mathbf{i}_s = [\,i_{sd}\;\; i_{sq}\,]^T$ the stator current, $\boldsymbol{\psi}_s = [\,\psi_{sd}\;\; \psi_{sq}\,]^T$ the stator flux, R_s the stator resistance, $\omega_m = \dot{\theta}_m$ the electrical angular speed of the rotor, and

$$\mathbf{J} = \begin{bmatrix} 0 & -1 \\ 1 & 0 \end{bmatrix}$$

The stator flux is

$$\boldsymbol{\psi}_s = \mathbf{L}_s\mathbf{i}_s + \boldsymbol{\psi}_{pm} \tag{2}$$

where $\boldsymbol{\psi}_{pm} = [\,\psi_{pm}\;\; 0\,]^T$ is the permanent magnet flux and

$$\mathbf{L}_s = \begin{bmatrix} L_d & 0 \\ 0 & L_q \end{bmatrix}$$

is the inductance matrix, L_d and L_q being the direct- and quadrature-axis inductances, respectively. The electromagnetic torque is given by

$$T_e = \frac{3p}{2}\boldsymbol{\psi}_s^T\mathbf{J}^T\mathbf{i}_s \tag{3}$$

where p is the number of pole pairs.

The LC filter equations are

$$\mathbf{u}_A - \mathbf{u}_s = R_{Lf}\mathbf{i}_A + L_f\dot{\mathbf{i}}_A + \omega_m L_f\mathbf{J}\mathbf{i}_A \tag{4}$$

$$\mathbf{i}_A - \mathbf{i}_s = C_f\dot{\mathbf{u}}_s + \omega_m C_f\mathbf{J}\mathbf{u}_s \tag{5}$$

where $\mathbf{i}_A = \begin{bmatrix} i_{Ad} & i_{Aq} \end{bmatrix}^T$ is the inverter current, $\mathbf{u}_A = \begin{bmatrix} u_{Ad} & u_{Aq} \end{bmatrix}^T$ the inverter output voltage, L_f the inductance and R_{Lf} the series resistance of the filter inductor, and C_f is the filter capacitance.

III. Control System

Fig. 2 shows a simplified block diagram of the control system (the estimated quantities being marked by the symbol $\hat{}$). The cascade control and speed-adaptive full-order observer are implemented in the estimated rotor reference frame. The estimated rotor position $\hat{\theta}_m$ is obtained by integrating $\hat{\omega}_m$. The inverter current, the stator voltage, and the stator current are controlled by PI controllers, and cross-couplings due to the rotating reference frame are compensated [7]. A maximum torque per current method is used for calculating the stator current reference [15]. The rotor speed is governed by a PI controller with active damping.

IV. Observer Structure

In the following, the speed-adaptive full-order observer proposed in [10] is augmented with an HF signal injection technique to stabilize the observer at low speeds. The two methods are combined in a fashion similar to [16]. The observer gain is modified for better compatibility with the HF signal injection method.

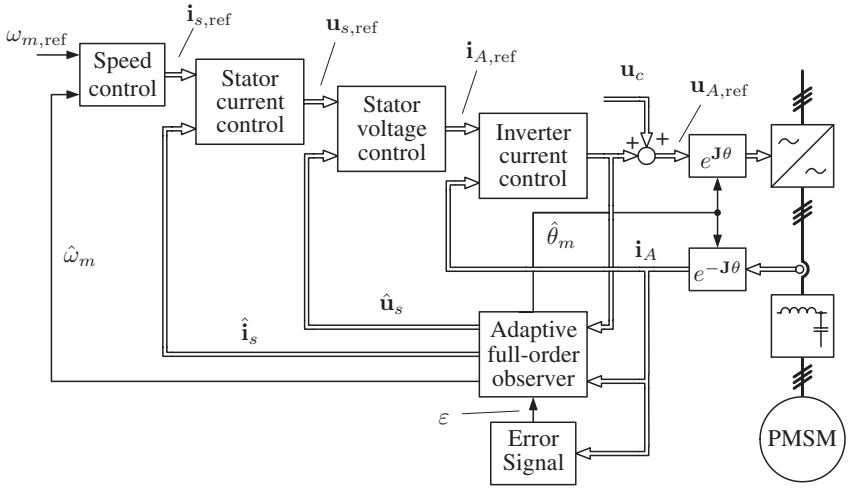

Fig. 2. Simplified block diagram of the control system. Double lines indicate vector quantities whereas single lines indicate scalar quantities. Vector quantities on the left-hand side of coordinate transformations are in the estimated rotor reference frame and on the right-hand side in the stator reference frame. The speed control includes the calculation of the stator current reference according to the maximum torque per current method.

A. High-Frequency Signal Injection

Various signal injection methods have been used for interior PMSMs. Discrete voltage pulses can be injected into the machine to detect the inductance variations [11]. Another alternative is to inject a continuous voltage signal into the motor. The voltage signal can either rotate in the stationary reference frame [12], or alternate in the estimated rotor reference frame [17]. The rotor position can be estimated by detecting the maximum and minimum points of the high-frequency current amplitude [13], or by demodulating the current signal in order to obtain an error signal proportional to the rotor position estimation error [12], [17]. An error signal can also be calculated as a difference between two squared high-frequency current components displaced from the d axis in opposite directions [14].

In this paper, an adaptive full-order observer is primarily used for the estimation. The HF signal injection method is used for a correction in the observer, and for that purpose, an error signal proportional to the rotor position estimation error is required. Alternating signal injection is preferred to rotating signal injection since the resulting HF torque ripple is lower. Demodulation of the current signal is chosen because it gives the best sensitivity in the case of the motor used in the experiments.

The HF signal injection method is based on [17]. A carrier excitation signal

$$\mathbf{u}_c = \hat{u}_c \cos(\omega_c t) \begin{bmatrix} 1 \\ 0 \end{bmatrix}, \tag{6}$$

having amplitude $\hat{u}_c$ and angular frequency ω_c, is superimposed on the inverter voltage reference in the estimated rotor reference frame. An HF current response is detected on the q axis of the estimated rotor reference frame, amplitude modulated by the rotor position estimation error. The q component of the measured current is band-pass filtered (BPF), giving an HF current signal i_{qc} that varies at the signal injection frequency. The current signal is then demodulated and low-pass filtered (LPF) to extract an error signal

$$\varepsilon = \mathrm{LPF}\big\{ i_{qc} \sin(\omega_c t) \big\} \tag{7}$$

This error signal is approximately

$$\varepsilon \approx K_\varepsilon \sin(2\tilde{\theta}_m) \tag{8}$$

where K_ε is the signal injection gain and $\tilde{\theta}_m = \theta_m - \hat{\theta}_m$ is the estimation error of the rotor position. Without the inverter output LC filter, the signal injection gain would be

$$K_\varepsilon = \frac{\hat{u}_c}{\omega_c} \frac{L_q - L_d}{4 L_q L_d} \tag{9}$$

The error signal ε is used as a correction in the adaptive full-order observer as will be described in Section IV-C.

A constant stator resistance and constant d- and q-axis inductances were used for the simulations presented in this paper. The PMSM used in the laboratory experiments has a laminated rotor with buried permanent magnets. The measured inductances of this motor type decrease with the frequency, but the inductance variations are small at frequencies below 1-2 kHz [18]. The influence of magnetic saturation on the experimental PMSM is negligible even if 150% of the nominal current is applied to the machine. In practice, the simulation results for signal injection methods, obtained using constant parameter values, correspond well to the experimental results [16], [19].

TABLE I
SYSTEM DATA

Motor Data	
Nominal voltage U_N	370 V
Nominal current I_N	4.3 A
Nominal frequency f_N	75 Hz
Nominal torque T_N	14.0 Nm
Stator resistance R_s	3.59 Ω
Direct-axis inductance L_d	0.036 H
Quadrature-axis inductance L_q	0.051 H
Permanent magnet flux ψ_{pm}	0.545 Vs
Total moment of inertia	0.015 kgm^2
LC Filter Parameters	
Inductance L_f	5.1 mH
Capacitance C_f	6.8 μF
Series resistance R_{Lf}	0.1 Ω
Control System Parameters	
Inverter current control bandwidth	2π·600 rad/s
Stator voltage control bandwidth	2π·400 rad/s
Stator current control bandwidth	2π·200 rad/s
Speed control bandwidth	2π·5 rad/s
Speed adaptation bandwidth α_{fo}	2π·100 rad/s
Bandwidth α_i at zero speed	2π·5 rad/s

B. Effect of the Filter on Signal Injection

It is not obvious that an LC filter can be used with HF signal injection. The authors have used the excitation frequency of 1 kHz in [16] and the frequency of 833 Hz in [20]. The parameters of the system are given in Table I. The resonance frequency of the filter is 855 Hz. On the d axis, the resonance frequency of the system is 913 Hz when the contribution of the d-axis inductance of the PMSM is taken into account. If a voltage having an amplitude of 40 V corresponding to [20] and a frequency of 1 kHz or 833 Hz is used with the filter, the resulting HF component of the inverter current exceeds the nominal current of the PMSM. Hence, the effect of the filter on the signal injection needs to be investigated.

To illustrate the effect of the filter on the HF signal injection, frequency responses of the system were calculated numerically. Parameters given in Table I were used for this example. The inverter d-axis current response to the inverter d-axis voltage is shown in Fig. 3(a) for the rotor position estimation error $\tilde{\theta}_m = 10^\circ$. The amplitude response has a notch at the parallel resonance frequency of the filter capacitor and the stator inductance, and a peak at the LC filter resonance frequency. Above the frequency $f \approx 500$ Hz, the LC filter amplifies the response as compared to the response obtained for the PMSM without the filter.

Fig. 3(b) shows the inverter q-axis current response to the inverter d-axis voltage for the rotor position estimation error $\tilde{\theta}_m = 10^\circ$. This response is important for the pulsating HF signal injection method, because the inverter q axis current is used for the demodulation. Compared to Fig. 3(a), the parallel resonance of the filter capacitance and the d-axis inductance

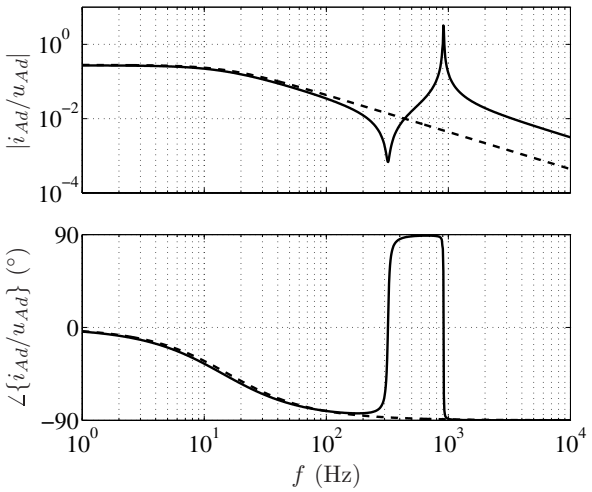

(a)

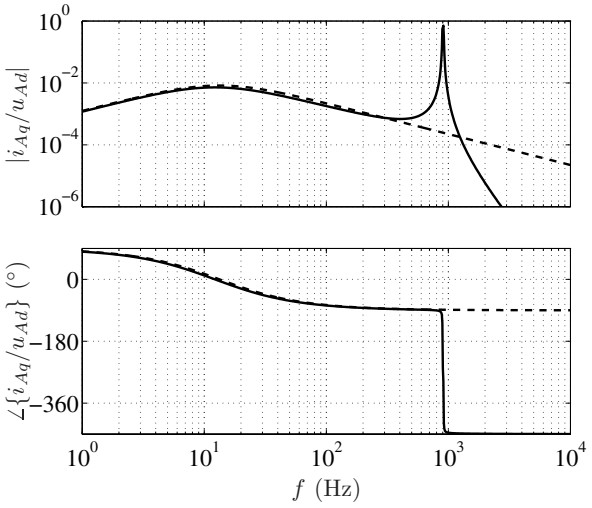

(b)

Fig. 3. Frequency responses of the system: (a) inverter d-axis current response to inverter d-axis voltage; (b) inverter q-axis current response to inverter d-axis voltage. Dashed lines show the response of the PMSM only, solid lines the response of LC filter and PMSM.

cannot be seen in the response, but the LC filter resonance peak is visible. At higher frequencies, the amplitude response decays rapidly.

The HF current amplitude on the q axis is approximately proportional to the estimation error $\tilde{\theta}_m$ of the rotor position for small values of $\tilde{\theta}_m$. Hence at $\tilde{\theta}_m = 1°$, for example, the amplitude response of the q-axis current is approximately 10% of that shown in Fig. 3(b), and $\tilde{\theta}_m = 0$ gives zero amplitude response. The phase response is unchanged for positive values of $\tilde{\theta}_m$, but it is shifted by 180° for negative values of $\tilde{\theta}_m$.

It is important that the excitation frequency is selected carefully. If the frequency is too low, the excitation disturbs the controllers. If the excitation frequency is above the resonance frequency of the filter, the inverter q axis current may be too low for reliable detection according to Fig. 3(b). If the excitation frequency is close to the resonance frequency of the filter, the stator voltage and the inverter current may become unacceptably high. It is reasonable to select the frequency of the carrier excitation signal below the resonance frequency. If the excitation frequency is selected close to the resonance frequency, the HF current amplitude, and hence also the signal injection gain K_ε, are increased by the LC filter. For the LC filter used in this paper, 500 Hz was selected for the excitation frequency, at which the filter increases the signal injection gain K_ε by a factor of 1.65 in this example.

C. Speed-Adaptive Full-Order Observer

The adaptive full-order observer is based on the dynamic models of the PMSM and the LC filter. The inverter current serves as the feedback signal for the observer, and the electrical angular speed of the rotor is estimated using an adaptation mechanism. The stator flux is selected as the state variable representing the electrical dynamics of the motor by inserting the stator current solved from (2) to (1). When the dynamic equations of the filter are included, the observer is defined by

$$\dot{\hat{\mathbf{x}}} = \hat{\mathbf{A}}\,\hat{\mathbf{x}} + \hat{\mathbf{B}} \begin{bmatrix} \mathbf{u}_A \\ \hat{\boldsymbol{\psi}}_{pm} \end{bmatrix} + \mathbf{K}(\mathbf{i}_A - \hat{\mathbf{i}}_A) \tag{10}$$

where $\hat{\mathbf{x}} = \begin{bmatrix} \hat{\mathbf{i}}_A^T & \hat{\mathbf{u}}_s^T & \hat{\boldsymbol{\psi}}_s{}^T \end{bmatrix}^T$. The inverter voltage $\mathbf{u}_A$ and the permanent magnet flux estimate $\hat{\boldsymbol{\psi}}_{pm}$ are considered as inputs to the system. The system matrices and the observer gain matrix in (10) are

$$\hat{\mathbf{A}} = \begin{bmatrix} -\hat{R}_{Lf}\hat{L}_f^{-1}\mathbf{I} & -\hat{L}_f^{-1}\mathbf{I} & \mathbf{0} \\ \hat{C}_f^{-1}\mathbf{I} & \mathbf{0} & -\hat{C}_f^{-1}\hat{\mathbf{L}}_s^{-1} \\ \mathbf{0} & \mathbf{I} & -\hat{R}_s\hat{\mathbf{L}}_s^{-1} \end{bmatrix} - (\hat{\omega}_m - \omega_\varepsilon) \begin{bmatrix} \mathbf{J} & \mathbf{0} & \mathbf{0} \\ \mathbf{0} & \mathbf{J} & \mathbf{0} \\ \mathbf{0} & \mathbf{0} & \mathbf{J} \end{bmatrix} \tag{11}$$

$$\hat{\mathbf{B}} = \begin{bmatrix} \hat{L}_f^{-1}\mathbf{I} & \mathbf{0} \\ \mathbf{0} & \hat{C}_f^{-1}\hat{\mathbf{L}}_s^{-1} \\ \mathbf{0} & \hat{R}_s\hat{\mathbf{L}}_s^{-1} \end{bmatrix} \tag{12}$$

$$\mathbf{K} = \begin{bmatrix} k_{1d}\mathbf{I} + k_{1q}\mathbf{J} \\ k_{2d}\mathbf{I} + k_{2q}\mathbf{J} \\ k_{3d}\mathbf{I} + k_{3q}\mathbf{J} \end{bmatrix} \tag{13}$$

respectively, where $\mathbf{I}$ is the 2x2 unit matrix. The factors k_{id} and k_{iq} ($i = 1,\ 2,\ 3$) are scalar gain parameters. The estimate for the stator current, required for the controller feedback, is calculated based on (2):

$$\hat{\mathbf{i}}_s = \hat{\mathbf{L}}_s^{-1}(\hat{\boldsymbol{\psi}}_s - \hat{\boldsymbol{\psi}}_{pm}) \tag{14}$$

The speed adaptation law is

$$\hat{\omega}_m = -k_p\,(i_{Aq} - \hat{i}_{Aq}) - k_i \int (i_{Aq} - \hat{i}_{Aq})dt \tag{15}$$

where k_p and k_i are nonnegative adaptation gains. According to [16], these gains are selected as

$$k_p = \frac{2\alpha_{fo}}{\hat{\psi}_{pm}/\hat{L}_q}, \quad k_i = \frac{\alpha_{fo}^2}{\hat{\psi}_{pm}/\hat{L}_q} \tag{16}$$

where the design parameter α_{fo} corresponds to the approximate bandwidth of the speed adaptation.

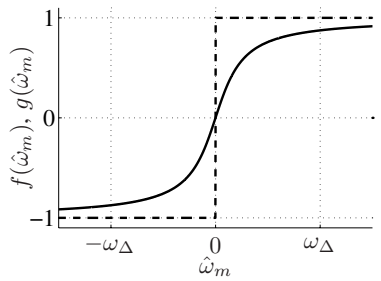

Fig. 4. Function $f(\hat{\omega}_m)$ (dotted), original function $g(\hat{\omega}_m)$ (dashed), and proposed function $g(\hat{\omega}_m)$ (solid) as functions of estimated rotor speed.

In (11), the speed correction term ω_ε is based on the HF signal injection method. It is obtained from the error signal ε by means of a PI mechanism

$$\omega_\varepsilon = \gamma_p \varepsilon + \gamma_i \int \varepsilon dt \tag{17}$$

where γ_p and γ_i are nonnegative gains. The gains are selected as [19]

$$\gamma_p = \frac{\alpha_i}{2K_\varepsilon}, \quad \gamma_i = \frac{\alpha_i^2}{6K_\varepsilon} \tag{18}$$

where α_i is the approximate bandwidth of the PI mechanism. In (18), the influence of the LC filter on the signal injection gain K_ε should be taken into account.

The effect of the signal injection method is reduced linearly as the rotor speed increases, reaching zero at the transition speed ω_Δ. Both the HF excitation voltage $\hat{u}_c$ and the approximate bandwidth α_i of the PI mechanism in (17) are decreased, i.e.

$$\hat{u}_c = f(\hat{\omega}_m)\hat{u}_{c0}, \quad \alpha_i = f(\hat{\omega}_m)\alpha_{i0} \tag{19}$$

where $\hat{u}_{c0}$ and α_{i0} are the zero-speed values of the HF excitation voltage and the PI mechanism bandwidth, respectively. The function $f(\hat{\omega}_m)$ is shown in Fig. 4 as a function of the estimated rotor speed.

In [10], the observer gain was selected as

$$\mathbf{K} = \begin{bmatrix} k_{1d}\mathbf{I} \\ \mathbf{0} \\ k_{3d}\mathbf{I} + k_{3q}\underbrace{\mathrm{sign}(\hat{\omega}_m)}_{g(\hat{\omega}_m)}\mathbf{J} \end{bmatrix} \tag{20}$$

When the observer is augmented with the signal injection method, however, zero-speed operation becomes unstable due to the discontinuity of the signum function. It is better to use a smoother speed-dependent function

$$\mathbf{K} = \begin{bmatrix} k_{1d}\mathbf{I} \\ \mathbf{0} \\ k_{3d}\mathbf{I} + k_{3q}\underbrace{(2/\pi)\mathrm{atan}(k_s\hat{\omega}_m/\omega_\Delta)}_{g(\hat{\omega}_m)}\mathbf{J} \end{bmatrix} \tag{21}$$

where k_s defines the steepness of the $g(\hat{\omega}_m)$ function. A value $k_s = 5$ is used in the following. This modification is illustrated in Fig. 4. The other gain parameters are $k_{1d} = 2000$ s^{-1} and $k_{3d} = k_{3q} = 2\hat{R}_s$.

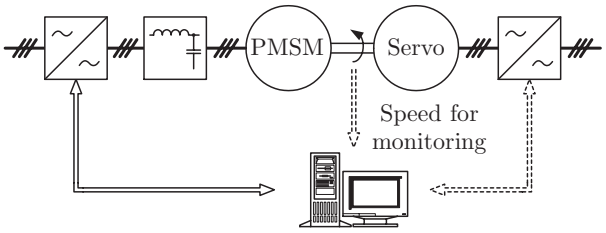

Fig. 5. Experimental setup. Mechanical load is provided by a servo drive.

V. Results

The proposed method was investigated by means of simulations and laboratory experiments. The data of the six-pole interior-magnet PMSM (2.2 kW, 1500 rpm) and the LC filter, and the cascade control bandwidths are given in Table I. The base values for the voltage, current, and angular speed are defined as $U_B = \sqrt{2/3}U_N$, $I_B = \sqrt{2}I_N$, and $\omega_B = 2\pi f_N$, respectively. The electromagnetic torque is limited to 22 Nm, which is 1.57 times the nominal torque T_N. The high-frequency carrier excitation signal has a frequency of 500 Hz and an amplitude of 30 V. The transition speed $\omega_\Delta = 0.13$ p.u. The digital implementation of the adaptive full-order observer is based on a simple symmetric Euler method [21], [7].

The experimental setup is illustrated in Fig. 5. The PMSM is fed through the LC filter by a frequency converter that is controlled by a dSpace DS1103 PPC/DSP board. Mechanical load is provided by a PMSM servo drive. An incremental encoder is used for monitoring the actual rotor speed and position. The nominal dc-link voltage is 540 V, and the switching frequency and the sampling frequency are both 5 kHz. The dc-link voltage of the converter is measured, and simple current feedforward compensation is applied for dead times and power device voltage drops [22].

The Matlab/Simulink environment was used for the simulations. The parameter values used in the controller were equal to those of the motor and filter models. Simulation and experimental results showing speed reference steps at zero load torque are depicted in Fig. 6. The rotor position estimation error shown in the last subplot is the difference between the actual (measured) and estimated values. This position estimation error is a good indicator of the estimation performance. The HF signal injection contributes to the rotor speed and position estimation at the speed ω_m = 0.05 p.u. The estimation accuracy for the rotor speed and position is good even at low speeds. The ripple in the measured results is caused by harmonics in the permanent magnet flux and in the motor inductances [20], and current measurement inaccuracies.

Fig. 7 shows simulation and experimental results at zero speed reference when nominal load torque steps are applied. The proposed observer is stable, both in transient and steady-state conditions. The rotor position estimation error stays small, indicating good dynamic properties. The steady-state rotor position estimation error is caused by spatial harmonics in the stator inductances [20]. This estimation error is a periodic function of the rotor position. Experimental results

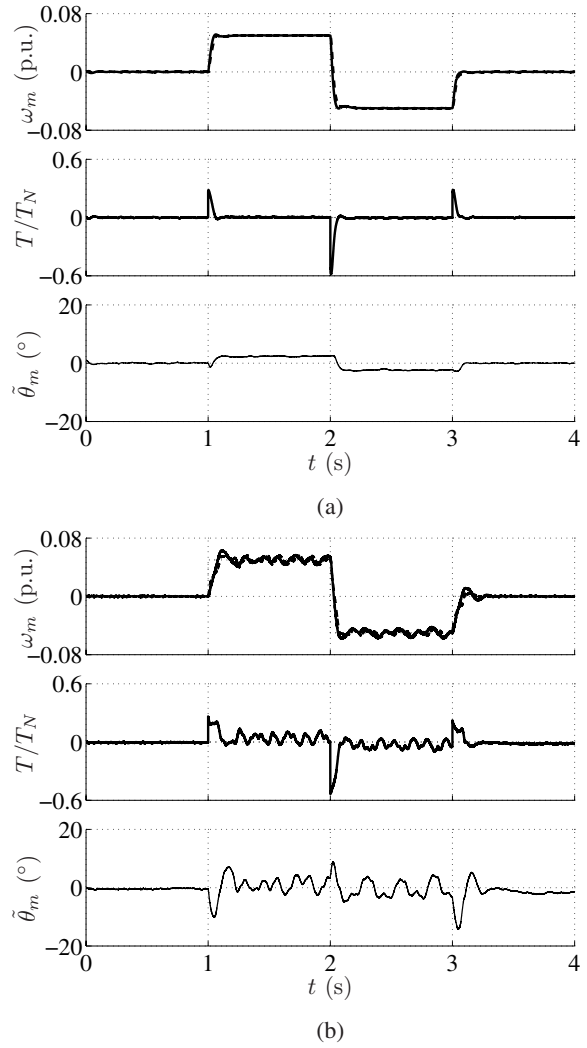

Fig. 6. Speed reference steps at no load: (a) simulation results; (b) experimental results. First subplot shows electrical angular speed (solid), its estimate (dashed), and its reference (dotted). Second subplot shows estimated electromagnetic torque (solid) and load torque reference (dotted). Last subplot shows estimation error of rotor position in electrical degrees.

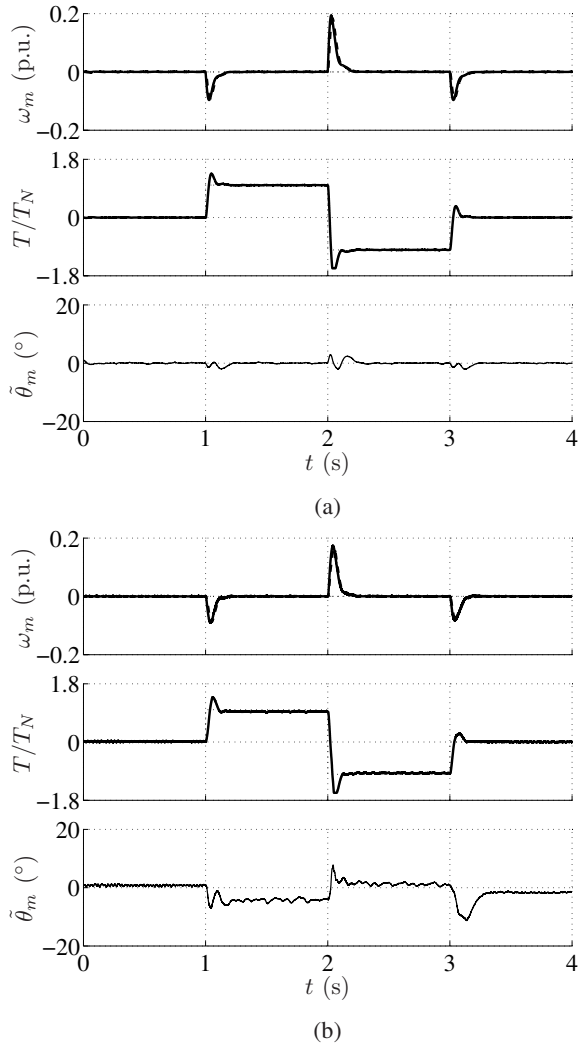

Fig. 7. Load torque steps at zero speed reference: (a) simulation results; (b) experimental results. Explanations of the curves are as in Fig. 6.

showing a slow speed reversal at nominal load torque are depicted in Fig. 8. The system is stable both in the motoring and regenerating modes of operation, and sustained operation at low speeds is possible.

VI. Conclusions

It is possible to use a signal injection method for the rotor speed and position estimation of PMSM drives even if an inverter output LC filter is used. According to the frequency-domain analysis shown in the paper, the excitation frequency of the signal injection should be selected carefully in order to avoid exciting the filter resonance. The signal injection method is used for augmenting an adaptive full-order observer at low speeds. The simulation and experimental results show that the proposed system can cope with stepwise changes in the speed reference and load torque. The performance of the proposed sensorless method is comparable to that of a PMSM drive without the LC filter.

VII. Acknowledgement

The authors would like to thank the reviewers for their professional work and helpful suggestions.

References

[1] Y. Murai, T. Kubota, and Y. Kawase, "Leakage current reduction for a high-frequency carrier inverter feeding an induction motor," *IEEE Trans. Ind. Appl.*, vol. 28, no. 4, pp. 858–863, July/Aug. 1992.

[2] M. Carpita, D. Colombo, A. Monti, and A. Fradilli, "Power converter filtering techniques design for very high speed drive systems," in *Proc. EPE'01*, Graz, Austria, Aug. 1991.

[3] T. D. Batzel and K. Y. Lee, "Electric propulsion with sensorless permanent magnet synchronous motor: implementation and performance," *IEEE Trans. Energy Convers.*, vol. 20, no. 3, pp. 575–583, Sep. 2005.

[4] J.-D. Park, C. Khalizadeh, and H. Hofmann, "Design and control of high-speed solid-rotor synchronous reluctance drive with three-phase LC filter," in *Conf. Rec. IEEE-IAS Annu. Meeting*, Hong Kong, China, Oct. 2005, pp. 715–722.

[5] W. Zimmermann, "Feldorientiert geregelter Umrichterantrieb mit sinusförmigen Maschinenspannungen," *etzArchiv*, vol. 10, no. 8, pp. 259–266, Aug. 1988.

[6] M. Kojima, K. Hirabayashi, Y. Kawabata, E. C. Ejiogu, and T. Kawabata, "Novel vector control system using deadbeat-controlled PWM inverter with output LC filter," *IEEE Trans. Ind. Appl.*, vol. 40, no. 1, pp. 162–169, Jan./Feb. 2004.

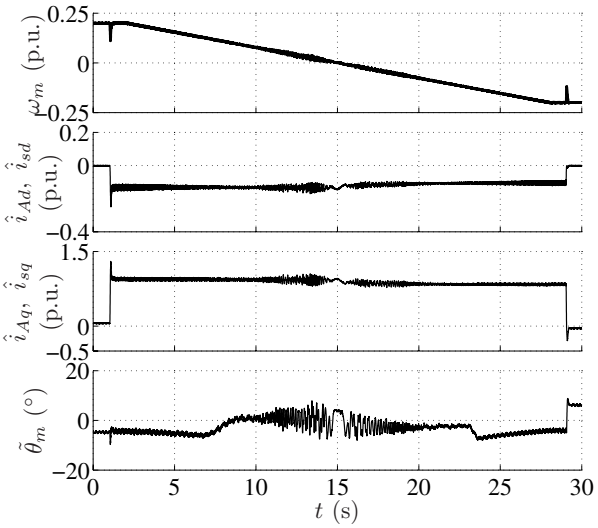

Fig. 8. Experimental results showing slow speed reversal at nominal load torque. First subplot shows electrical angular speed (solid), its estimate (dashed), and its reference (dotted). Second subplot shows estimated stator d-axis current, and third subplot estimated stator q-axis current. Last subplot shows estimation error of rotor position in electrical degrees.

[7] J. Salomäki and J. Luomi, "Vector control of an induction motor fed by a PWM inverter with output LC filter," *EPE Journal*, vol. 16, no. 1, pp. 37–43, 2006.

[8] J. Salomäki, M. Hinkkanen, and J. Luomi, "Sensorless vector control of an induction motor fed by a PWM inverter through an output LC filter," *Trans. IEEJ*, vol. 126-D, no. 4, pp. 430–437, Apr. 2006.

[9] ——, "Sensorless control of induction motor drives equipped with inverter output filter," *IEEE Trans. Ind. Electron.*, vol. 53, no. 4, Aug. 2006.

[10] J. Salomäki, A. Piippo, M. Hinkkanen, and J. Luomi, "Sensorless vector control of PMSM drives equipped with inverter output filter," in *Proc. IEEE IECON'06*, Paris, France, Nov. 2006, pp. 1059–1064.

[11] M. Schroedl, "Sensorless control of AC machines at low speed and standstill based on the INFORM method," in *Conf. Rec. IEEE-IAS Annu. Meeting*, vol. 1, San Diego, CA, Oct. 1996, pp. 270–277.

[12] P. L. Jansen and R. D. Lorenz, "Transducerless position and velocity estimation in induction and salient AC machines," *IEEE Trans. Ind. Applicat.*, vol. 31, no. 2, pp. 240–247, March/April 1995.

[13] A. Consoli, G. Scarcella, and A. Testa, "Industry application of zero-speed sensorless control techniques for PM synchronous motors," *IEEE Trans. Ind. Applicat.*, vol. 37, no. 2, pp. 513–521, March/April 2001.

[14] J. I. Ha, K. Ide, T. Sawa, and S. K. Sul, "Sensorless rotor position estimation of an interior permanent-magnet motor from initial states," *IEEE Trans. Ind. Applicat.*, vol. 39, no. 3, pp. 761–767, May/June 2003.

[15] T. Jahns, G. Kliman, and T. Neumann, "Interior permanent-magnet synchronous motors for adjustable-speed drives," *IEEE Trans. Ind. Applicat.*, vol. 22, no. 4, pp. 738–747, July/Aug. 1986.

[16] A. Piippo and J. Luomi, "Adaptive observer combined with HF signal injection for sensorless control of PMSM drives," in *Proc. IEEE IEMDC'05*, San Antonio, TX, May 2005, pp. 674–681.

[17] M. Corley and R. D. Lorenz, "Rotor position and velocity estimation for a salient-pole permanent magnet synchronous machine at standstill and high speeds," *IEEE Trans. Ind. Applicat.*, vol. 43, no. 4, pp. 784–789, July/Aug. 1998.

[18] S. Øvrebø, "Sensorless control of permanent magnet synchronous machines," Doct. thesis, Norwegian University of Science and Technology, 2004.

[19] A. Piippo, M. Hinkkanen, and J. Luomi, "Sensorless control of PMSM drives using a combination of voltage model and HF signal injection," in *Conf. Rec. IEEE-IAS Annu. Meeting*, vol. 2, Seattle, WA, Oct. 2004, pp. 964–970.

[20] A. Piippo and J. Luomi, "Inductance harmonics in permanent magnet synchronous motors and reduction of their effects in sensorless control," in *Proc. ICEM/2006*, no. 138, Chania, Greece, Sept. 2006, CD-ROM.

[21] J. Niiranen, "Fast and accurate symmetric Euler algorithm for electromechanical simulations," in *Proc. Electrimacs'99*, vol. 1, Lisboa, Portugal, Sept. 1999, pp. 71–78.

[22] J. K. Pedersen, F. Blaabjerg, J. W. Jensen, and P. Thogersen, "An ideal PWM-VSI inverter with feedforward and feedback compensation," in *Proc. EPE'93*, vol. 5, Brighton, UK, Sept. 1993, pp. 501–507.

AUTHORS' BIOGRAPHIES

Antti Piippo is a Design Engineer at ABB Oy, Helsinki, Finland. In 2003, he joined Helsinki University of Technology, where he worked as a research scientist at the Power Electronics Laboratory until 2007. His current research interests include the control of synchronous motor drives. He received the M.Sc. (Eng.) degree from Helsinki University of Technology in 2003.

Janne Salomäki (M'08) is currently an R&D Engineer at Konecranes, Hyvinkää, Finland. In 2003, he joined Helsinki University of Technology, where he worked as a Researcher at the Power Electronics Laboratory until 2007. His current research interests include the control of electric drives in crane applications. He received the M.Sc.(Eng.) and D.Sc.(Tech.) degrees from Helsinki University of Technology, Espoo, Finland, in 2003 and 2007, respectively.

Jorma Luomi (M'92) is a Professor in the Department of Electrical Engineering, Helsinki University of Technology, Espoo, Finland. He joined Helsinki University of Technology in 1980, and from 1991 to 1998 he was a Professor at Chalmers University of Technology. His research interests are in the areas of electric drives, electric machines, and numerical analysis of electromagnetic fields. He received the M.Sc.(Eng.) and D.Sc.(Tech.) degrees from Helsinki University of Technology, in 1977 and 1984, respectively.